Research Article

Journal of Molecular Recognition

Received: 10 December 2012, Revised: 4 March 2013, Accepted: 9 April 2013, Published online in Wiley Online Library

(wileyonlinelibrary.com) DOI: 10.1002/jmr.2278

Nanostructure shape effects on response of plasmonic aptamer sensors

Subramanian Balamurugan[c], Kathryn M. Mayer[a], Seunghyun Lee[a], Steven A. Soper[c], Jason H. Hafner[a,b]* and David A. Spivak[c]*

A localized surface plasmon resonance (LSPR) sensor surface was fabricated by the deposition of gold nanorods on a glass substrate and subsequent immobilization of the DNA aptamer, which specifically bind to thrombin. This LSPR aptamer sensor showed a response of 6-nm λ_{max} shift for protein binding with the detection limit of at least 10 pM, indicating one of the highest sensitivities achieved for thrombin detection by optical extinction LSPR. We also tested the LSPR sensor fabricated using gold bipyramid, which showed higher refractive index sensitivity than the gold nanorods, but the overall response of gold bipyramid sensor appears to be 25% less than that of the gold nanorod substrate, despite the approximately twofold higher refractive index sensitivity. XPS analysis showed that this is due to the low surface density of aptamers on the gold bipyramid compared with gold nanorods. The low surface density of the aptamers on the gold bipyramid surface may be due to the effect of shape of the nanostructure on the kinetics of aptamer monolayer formation. The small size of aptamers relative to other bioreceptors is the key to achieving high sensitivity by biosensors on the basis of LSPR, demonstrated here for protein binding. The generality of aptamer sensors for protein detection using gold nanorod and gold nanobipyramid substrates is anticipated to have a large impact in the important development of sensors toward biomarkers, environmental toxins, and warfare agents. Copyright © 2013 John Wiley & Sons, Ltd.

Supporting information may be found in the online version of this paper.

Keywords: aptamer; localized surface plasmon resonance; gold nanorod; gold nanopyramid; protein recognition; biosensor

INTRODUCTION

Upon irradiation with light, the free conduction electrons of the metallic nanostructures oscillate collectively, known as surface plasmon, because of its interaction with the light's electric field, with a resonant frequency that depends on the nanoparticles' size, shape, and composition (Mayer and Hafner, 2011). When the resonance conditions are met, the incident photon resonates with the surface plasmon, which leads to the absorbance and scattering of the incident light (Anker *et al*., 2008). Resonance and, hence, the wavelength of absorption depends on the nature of the metal, size of the nanostructure, its aspect ratio and the local dielectric environment around the nanostructure, which can be summed as the refractive index of the surrounding medium (Anker *et al*., 2008). For example, 13-nm gold nanoparticles show one absorption band in water at 520 nm (Storhoff *et al*., 1998). Other metallic nanostructures such as gold and silver nanorods and other shapes show two peaks, one peak due to resonance between lateral modes with light and one for resonance due to the longitudal modes that is tunable from the visible through the near infrared, depending on the nanorod aspect ratio (Mayer and Hafner, 2011).

Like surface plasmon resonance (SPR), localized surface plasmon resonance (LSPR) can measure the changes in the local refractive index, which results in the concomitant shift in the λ_{max} in the extinction spectra (Zhao *et al*., 2006; Mayer and Hafner, 2011). Using this property, a number of LSPR sensors using gold nanoparticles have been reported for measuring antigen–antibody interactions (Endo *et al*., 2005; Endo *et al*., 2006; Yu and Irudayaraj, 2007; Anker *et al*., 2008; Mayer *et al*., 2008), biotin–streptavidin interactions (Nath and Chilkoti, 2002; Marinakos *et al*., 2007; Nusz *et al*., 2008), and concanavalin A–protein interactions (Yonzon *et al*., 2004) and for the detection of organophosphorous pesticide (Lin *et al*., 2006) by measuring changes in the λ_{max} values. Unlike SPR, LSPR has a higher sensitivity to refractive index changes very close to the surface, within a range of 5–15 nm from the nanostructure surface (Haes and Van Duyne, 2004), compared with approximately 200–300 nm from metal film surface in SPR (Jung *et al*., 1998). In both cases, the sensitivity decreases exponentially from the surface (Haes *et al*., 2004). Thus, the sensitivity of the LSPR biosensor can be increased by using a small bioreceptor on the surface placing the binding event close to the surface. Another way to increase the sensitivity is by using nanostructures that show high λ_{max} shift for the unit change in the refractive index of the surroundings, known as refractive index sensitivity. In earlier work on LSPR sensors, gold nanoparticles were used as a sensor element (Nath and Chilkoti, 2002; Kitano *et al*., 2006). Recently, other

* *Correspondence to: David A. Spivak, Department of Chemistry, Louisiana State University, Baton Rouge, LA 70803, USA. E-mail: dspivak@lsu.edu*
Jason H. Hafner, Department of Chemistry, Rice University, Houston, TX 77005, USA. E-mail: hafner@rice.edu

a *K. M. Mayer, S. Lee, J. H. Hafner*
Department of Physics and Astronomy, Rice University, Houston, TX, 77005, USA

b *J. H. Hafner*
Department of Chemistry, Rice University, Houston, TX, 77005, USA

c *S. Balamurugan, S. A. Soper, D. A. Spivak*
Department of Chemistry, Louisiana State University, Baton Rouge, LA, 70803, USA

nanostructures such as nanorods and nanobipyramids exhibiting higher refractive sensitivity than spherical gold nanoparticles were used as the LSPR substrate (Mayer *et al*., 2008; Lee *et al*., 2009).

Aptamers are oligonucleotides that are specifically selected to bind to its target molecules by an *in vitro* combinatorial process called SELEX, Systematic Evolution of Ligands by Exponential Enrichment (Ellington and Szostak, 1990; Tuerk and Gold, 1990). Aptamers are either RNA or DNA and normally contains 15–60 nucleotide sequences. Aptamers have been selected for a wide range of molecules including small organic molecules (Baker *et al*., 2006), metal ions (Qin *et al*., 2010), chemical warfare agents (Lamont *et al*., 2011), proteins (Song *et al*., 2008), and whole cells (Meyer *et al*., 2011). Several reviews have been published that report important details of these artificial receptors and the processes for evolving them (Jayasena, 1999; Brody and Gold, 2000; Nimjee *et al*., 2005). Aptamers show high affinity and selectivity that is traditionally associated with proteins such as antibodies and recently increasingly used for the fabrication of biosensors (Jayasena, 1999; Brody and Gold, 2000; Nimjee *et al*., 2005). These artificial antibodies are small compared with antibodies and can immobilize directly on the gold nanostructures via end functional group in a particular orientation using a number of bioconjugation routes (Balamurugan *et al*., 2008a). These small receptors are expected to increase the sensitivity of the LSPR compared with antibody-based LSPR sensors by binding the target close to the gold surface. Surface immobilized DNA aptamers that bind thrombin have been used by our group (Balamurugan *et al*., 2006; Balamurugan *et al*., 2008b) and by others (Song *et al*., 2008) for biosensor development, and it has shown that these surface immobilized aptamers exhibit very good protein detection (Balamurugan *et al*., 2006; Song *et al*., 2008). Kim *et al*. reported an aptamer-sandwich LSPR sensor by immobilizing the aptamer on the surface fabricated by gold coating on porous alumina (Kim *et al*., 2008). Guo *et al*. showed that a thrombin binding aptamer immobilized on a gold nanorod exhibited excellent response to thrombin using single particle scattering measurements (Guo and Kim, 2011; Guo *et al*., 2011a, 2011b). More recently, Yasun *et al*. reported aptamer-modified gold nanorods for enrichment of rare proteins and detection using gel electrophoresis (Yasun *et al*., 2012). We report here the direct sensing by LSPR of thrombin by aptamers (Bock *et al*., 1992) immobilized on the surfaces of gold nanorod and gold bipyramid nanostructures. Because of the compact structure of the aptamer, it is shown that capture of the target protein is positioned optimally for maximum LSPR signal affording detection of picomole concentrations of thrombin.

EXPERIMENTAL

Materials

Modified DNA aptamer (5′ HS-$(CH_2)_6$-$(CH_2CH_2O)_6$-TTTTT-GGTT GGTGTGGTTGG 3′) was obtained from Eurogentec North America, San Diego, CA. (11-Mercaptoundecyl)triethyleneglycol (EG_3SH) was obtained from Sensopath Technologies, Bozeman, MT. Hydrogen tetrachloroaurate (III), cetyltrimethylammonium bromide (CTAB), aminopropyltriethoxysilane (APTES), mercaptohexadecanoic acid, and mercaptoundecanol were obtained from Sigma-Aldrich, St. Louis, MO. Sodium borohydride and silver nitrate were obtained from Acros Organics, Pittsburgh, PA. Ascorbic acid was obtained from Fisher Scientific, Waltham, MA., and methoxy poly(ethylene glycol) (mPEG-SH, average molecular weight 5000) (CH_3O-$(CH_2CH_2O)n$-CH_2CH_2-SH, $n \sim 110$) was obtained from Nektar Therapeutics, San Francisco, CA.

Preparation of gold nanorod solution

Gold nanorods were grown from a gold nanoparticle seed solution prepared using sodium borohydride reduction of hydrogen tetrachloroaurate (III) in the presence of the surfactant CTAB (Mayer *et al*., 2008). This seed solution was added to a nanorod growth solution consisting of 425 ml of 100 mM CTAB, 18 ml of 10 mM hydrogen tetrachloroaurate (III), 2.7 ml of 10 mM silver nitrate, and 2.9 ml of 100 mM ascorbic acid.

Preparation of gold bipyramid solution

The gold bipyramid was prepared as reported earlier using sodium citrate-stabilized gold seed particles (Lee *et al*., 2009). Bipyramids were grown using 0.5 ml of 10 mM hydrogen tetrachloroaurate (III) and 10 ml of 100 mM CTAB mixed with 0.1 ml of 10 mM silver nitrate solution. Sequentially, 0.2 ml of 1.0 M HCl and 0.08 ml of 100 mM ascorbic acid were added to the solution, and the seed solution was added. The volume of seed solution was varied between 15 and 50 μl to synthesize different sizes of gold bipyramids. These solutions were kept at 28 °C for several hours. During this time, the color changed gradually from almost clear to dark pink, with most of the color change occurring in the first hour.

Preparation of DNA aptamer monolayer on gold nanorod and gold bipyramid coated glass substrate

The gold nanorods were deposited on the clean glass microscopic slide using a procedure reported earlier (Mayer *et al*., 2008). First, the clean glass slides were immersed overnight in a 5-mM APTES solution in ethanol, rinsed with water, and dried under the flow of dry nitrogen. The APTES coated glass slides were then immersed in a PEGylated nanorod solution overnight. Then, the slides were rinsed and dried, and a uniform layer of gold nanorods remained on the surface with an absorbance of approximately 0.1 at the LSPR peak wavelength. The gold bipyramid substrates were also prepared using the same procedure (Lee *et al*., 2009). The CTAB-stabilized gold nanostructures (nanorods and bipyramids) were PEGylated using a process described previously (Liao and Hafner, 2005) by suspension in thiolated PEG solution for 12 hr.

Formation of mixed DNA aptamer monolayer on gold nanostructures

Glass substrates coated with gold nanorod as well as gold bipyramid were subjected to an oxygen plasma cleaner at low power for 30 sec in 200 mT oxygen (model PDC- 32G, Harrick Scientific) then rinsed with ethanol, water and briefly dried in a stream of dry nitrogen. The cleaned LSPR substrates were immersed in 1 μM solutions of an aptamer thiol (5′-HS-$(CH_2)_6$-$(CH_2CH_2O)_6$-TTTTT-GGTTGGTGTGGTTGG-3′) solution in 1 M potassium phosphate solution (pH 8) for 2 hr, then rinsed with deionized water and briefly dried in a stream of dry nitrogen. Immersion of these substrates in 10 mM of $HS(CH_2)_{11}(OCH_2CH_2)_3OH$ (EG_3-OH) solution in ethanol for 2 hr, rinsing with ethanol and then water, and drying in a stream of dry nitrogen covered the remaining bare gold with EG_3-OH (Balamurugan *et al*., 2006).

Measurement of thrombin binding on aptamer functionalized gold nanorod and gold bipyramid substrates

The LSPR spectra were measured using a closed flow cell assembly outlined in Scheme 1 (Mayer *et al.*, 2008) consisting of a glass slide coated with gold nanorod substrate and functionalized with mixed aptamer monolayer on one side and a clean glass slide on the other side separated with a 1.5-mm-thick polydimethylsiloxane (PDMS). Two holes were drilled to connect the input and output flows, and the PDMS sheet provided a 1 cm × 2 cm slot that served as the flow volume. This flow cell was mounted vertically on an optical bench in between a quartz–tungsten–halogen light source with collimating lens and a portable spectrometer (Ocean Optics USB4000) (Mayer *et al.*, 2008). A flow rate of 400 μl/min was controlled by a syringe pump (NE1000, New Era Pump Systems).

After equilibration with PBS buffer, thrombin solution at the desired concentration was contacted with a sensor surface under flow conditions. Absorbance spectra were collected continuously with averaging every 30 sec and recorded. Each spectrum was then analyzed in MATLAB with a Gaussian fit to monitor the peak wavelength, height, and width versus time. Once there was no further change in the λ_{max}, the next thrombin solution of higher concentration was introduced to the cell, and this process was repeated for all the thrombin solution concentrations (Mayer *et al.*, 2008). The data collection time for each thrombin concentration was approximately 20 min.

Surface characterization

The SEM images were obtained using FEI Quanta 3D FEB Scanning electron microscope (SEM). The XPS analysis was carried out in a Kratos XPS instrument (Balamurugan *et al.*, 2006).

RESULTS AND DISCUSSION

Thrombin sensor using rod-shaped gold nanostructure substrates

The gold nanorods used in these experiments were prepared from a solution of $HAuCl_4$ containing gold seed particles in the presence of CTAB using reported procedure (Nikoobakht and El-Sayed, 2003; Sau and Murphy, 2004). The CTAB acts both as the source of anisotropic growth to control final particle shape and as the stabilizer (Gao *et al.*, 2003). Thus, nanorods are formed with a weakly bound cationic bilayer on the nanorods surfaces (Sau and Murphy, 2005). Subsequently, thiol terminated PEG (polyethylene glycol, mw = 5000) is added, which exchanges with the CTAB to form stable nanorods in the solution (Liao and Hafner, 2005). The extinction spectrum of the gold nanorods (Figure 1) show two peaks, one at 509 nm (transverse resonance) and another at 680 nm (longitudinal resonance) (Mayer *et al.*, 2008). Comparison of the UV–vis and SEM data (Figure 1) with the previous data shows the dimensions of the nanorods as 18 ± 3 nm diameter, 44 ± 5 nm length, with the aspect ratio of 3.3 (Liao and Hafner, 2005). The refractive index sensitivity of these gold nanorods is 170 nm/RIU, and the figure of merit (sensitivity/line width) is 1.36 (Mayer *et al.*, 2008). The figure of merit of 1.36 is similar to the values reported for the other nanostructure ensembles (Liao *et al.*, 2006).

Plasma treatment of the immobilized nanorod surface removes the PEG layer from the nanorods, leaving a bare gold surface that can be functionalized with thiol-linked aptamers.

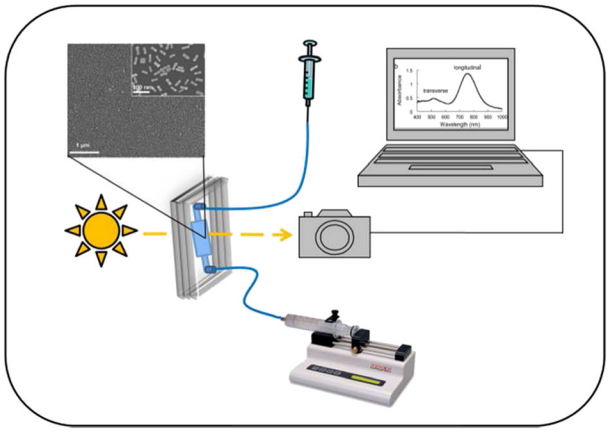

Scheme 1. Illustration of the LSPR closed cell apparatus used to obtain extinction spectra.

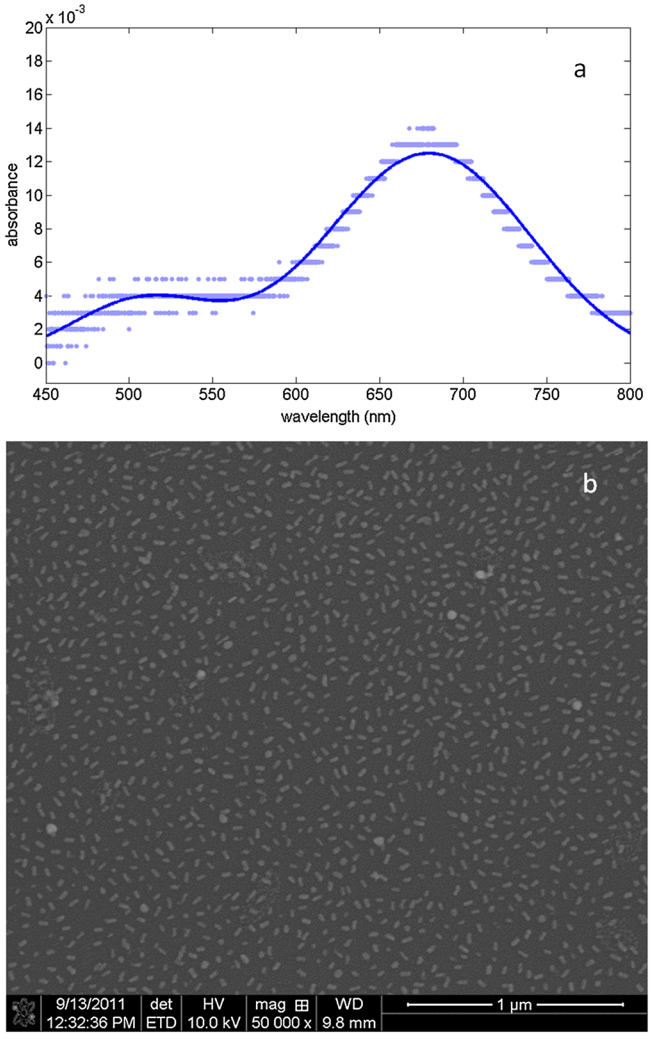

Figure 1. (a) The extinction spectra of the nanorod-coated substrate in the presence of PBS buffer. The light blue data is the raw data from the spectrometer, and the overlaid dark blue line is a fit to the data (the fitted function is the sum of two Gaussians). (b) SEM picture of the gold nanorods deposited on the glass substrate and subsequently functionalized with mixed aptamer monolayer.

This step does not affect the adhesion of gold nanorod to the glass surface as seen from the SEM image; however, plasma cleaning does cause a small LSPR blue shift consistent with the removal of a PEG layer (Mayer *et al.*, 2008). Earlier, we reported the optimized conditions for the formation of two-component aptamer monolayer using thiol-terminated aptamer and thiol terminated oligo-ethylene glycol (Balamurugan *et al.*, 2006; Balamurugan *et al.*, 2008b). The binding performance of the surface-immobilized aptamer was found to be dependent on the size and chemical nature of the linkers of both components. Use of hexaethyleneglycol units in the aptamer linker increased the thrombin binding, and the hexaethyleneglycol units in the co-adsorbent reduce the non-specific protein adsorption (Balamurugan *et al.*, 2006). The aptamer sequence incorporated five or 10 additional thymine units along with the hexaethyleneglycol unit as a linker to reduce the steric hindrance of the approaching thrombin protein and afforded maximum protein binding to the surface (Balamurugan *et al.*, 2008b). Hence, a mixed aptamer monolayer was formed on the gold nanorod substrate using 5′-HS-$(CH_2)_6$-$(OCH_2CH_2)_6$-TTTTT-GGTTGGTGTGGTTGG and HS$(CH_2)_{11}(OCH_2CH_2)_3$OH (EG_3-OH) thiols using the procedure described in the Experimental section (Balamurugan *et al.*, 2006).

Figure 2a shows the plot of maximum λ_{max} shift measured as a function of thrombin concentration. Continuous collection of spectra repeated every 30 sec allows fitting error to be determined as approximately $<$0.1 nm by measuring the wavelength changes during the stabilization period at each step at each concentration. The inset shows the individual spectra obtained for different concentrations of thrombin. The data show that this LSPR aptamer sensor detects the thrombin in the concentration range of 10 pM to 1 μM. This concentration range was better than the one detected by the SPR sensor surface functionalized with the aptamer monolayer under the same condition. The SPR sensor surface detects the thrombin in the concentration range of 1 nM to 1 μM (Balamurugan *et al.*, 2006). Further, these data also show that this LSPR sensor shows a λ_{max} shift of 6 nm (677.8–683.8 nm) for thrombin binding.

Recently, Kim and coworkers reported an aptamer functionalized single gold nanorod LSPR sensor (Guo and Kim, 2011; Guo *et al.*, 2011a, 2011b). The authors used scattering data, a method which provides low detection limits of analytes compared with using the λ_{max} shift in extinction spectra; this is due to the low S/N ratio of scattering measurements. The response of the thrombin aptamer-based sensor surface reported here has been measured to a lower limit of detection at 10 pM, compared with 250 pM in the system of Kim and coworkers (Guo and Kim, 2011; Guo *et al.*, 2011a, 2011b). Furthermore, the aptamer detection reported here exhibits a highly sensitive and linear response in the lower thrombin concentration range of ~10^{-10}–10^{-5} g/ml compared with the previously reported system (~10^{-8} to 10^{-6} g/ml) (Guo and Kim, 2011; Guo *et al.*, 2011a, 2011b).

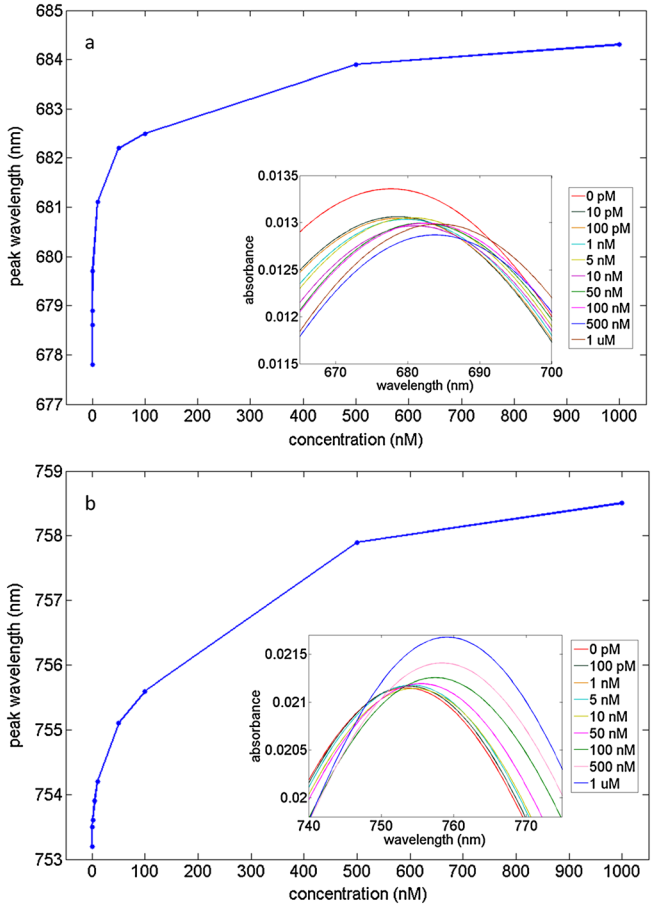

Figure 2. The figures show the plot of λ_{max} obtained for different concentrations of thrombin for (a) gold nanorod substrates and (b) gold bipyramid substrates. The inset shows the UV–vis spectrum obtained for increasing concentrations of thrombin.

Thrombin binding on gold bipyramid substrate

Gold bipyramids are nanoparticles with a penta-twinned crystal structure that have been shown to have sharp LSPR signals (Liu and Guyot-Sionnest, 2005). Earlier, the refractive index sensitivity of these gold bipyramid structures was reported to be 327 nm/RIU with a figure of merit (sensitivity/line width) of 3.7 (Lee *et al.*, 2009). Thus, LSPR sensors fabricated using these structures have potential for even higher sensitivity of thrombin detection than by nanorods such as those described above. The seed-mediated gold bipyramid structure was synthesized using a procedure reported earlier (Lee *et al.*, 2009). In this study, gold bipyramids of length 94 ± 11 nm and diameter 46 ± 6 nm were employed; the extinction spectra and SEM pictures are shown in Figure 3. A closer examination of the SEM picture shows that the sensor surface contains both nanobipyramids and nanoparticles. It was earlier reported that only 22% of the nanostructures on the glass substrate were nanobipyramids, and the rest were nanospheres (Lee *et al.*, 2009). In addition, the extinction spectra showed a strong peak at 560 nm, and although a peak at this position was expected because of the lateral modes of the bipyramid, the peak intensity should be less than the longitudal modes similar to the extinction spectra for gold nanorods (Figure 1). Thus, the peak at 560 nm in the extinction spectra for the nanobipyramid-coated surface (Figure 3) is the combined result of lateral modes of the gold bipyramid and response from the gold nanoparticles. Mixed aptamer monolayer was formed on the gold bipyramids employing the same procedure used for the functionalization of gold nanorods.

Looking at Figure 2b, the maximum λ_{max} shift of the aptamer-coated bipyramids increases as the concentration increases and levels off around 500 nM thrombin. This trend is similar to the concentration dependence for nanorods in Figure 2a; however, the overall response appears to be 25% less than that of the gold nanorod substrate, despite the approximately twofold higher

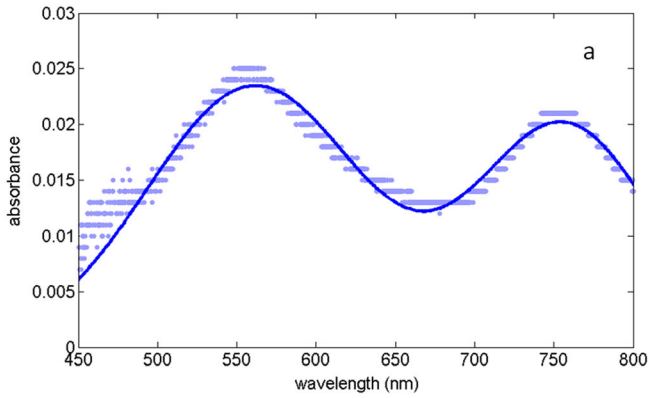

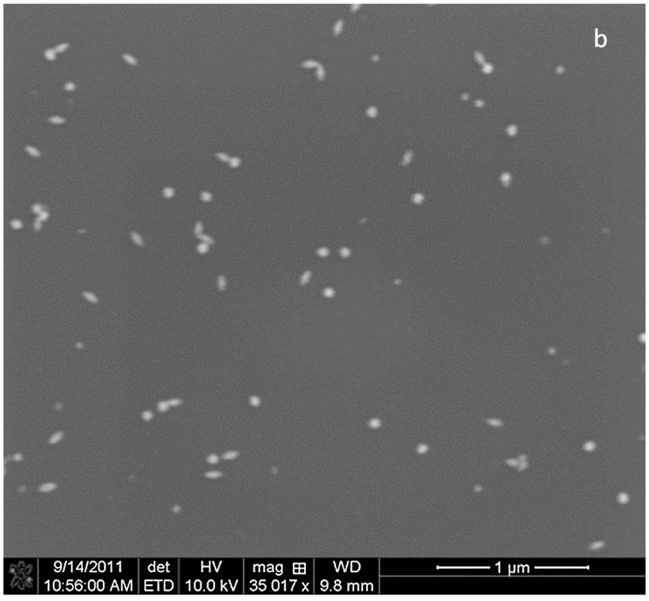

Figure 3. The extinction spectra (a) and the SEM picture (b) of the gold bipyramids immobilized on a glass substrate and functionalized with mixed aptamer monolayer.

Table 1. XPS analysis of relative surface density of aptamer on gold nanorods versus bipyramids after aptamer/EG_3-OH mixed monolayer formation

	Au4f/Si2p ratio	N1s/Au4f ratio
Gold nanorods substrate	0.1085	0.3845
Gold bipyramids substrate	0.01885	0.2072[a]

[a]Corrected for the fact that only 22% of the nanostructure on the glass substrate were the nanobipyramids and the rest were nanospheres (Lee *et al*., 2009). There is no LSPR signal from the spherical component above 350 nm.

refractive index sensitivity reported for gold bipyramids versus nanorods (327 nm/RIU vs 170 nm/RIU). This result is not explained by the lower density of gold bipyramids on the glass slide (Figure 1b versus 3b), because the lower surface density of nanobipyramids on the glass slide results only in lower intensity values of the spectra but does not change the magnitude of the spectral shift used for the LSPR detection values. Instead, the spectral shift is dependent on the amount of thrombin bound to the gold bipyramid surface, which in turn is dependent on the surface density of the aptamer. To determine the relative surface density of aptamer on nanorods versus bipyramids, XPS analysis (Table 1) was conducted, which revealed that the surface density of aptamer (as measured by N1s/Au4f ratio) on gold bipyramids is 54% less than on gold nanorods. This is the surface density value obtained after accounting for the aptamer on the gold particles that are present on the gold bipyramid-coated surface. The low surface density of the aptamer on the gold nanobipyramids compared with the gold nanorods under the same experimental conditions may be due to the effect of nanostructure shape on the kinetics of aptamer monolayer formation (Millstone *et al*., 2008).

It can be concluded that while the refractive index sensitivity is 1.92-fold higher for the bipyramids versus the nanorods, the surface coverage of aptamer on bipyramids is only 54% that of the nanorods. Thus, the higher refractive index sensitivity of the gold bipyramid was offset by the lower surface density of aptamer on its surface resulting in a negligible overall difference in response expected for the bipyramid sensor versus the nanorod sensor. The 25% lower response of the nanobipyramid versus the nanorod substrate (4.5 nm/6.0 nm) may be due to variations in the refractive index sensitivity, which depends on the location of attachment of the aptamer on the gold nanopyramid. Field enhancement is greatest at the tips of the nanobipyramid (Mayer *et al*., 2010); however, the population of immobilized aptamers is greatest away from the tips (especially at low aptamer coverage) (Millstone *et al*., 2008), lowering the overall effective value of the refractive index sensitivity.

CONCLUSIONS

The utility of aptamers for LSPR applications is amplified by the high sensitivity to protein binding, which can be attributed to the relatively compact size of the aptamer. Thus, the integration of aptamers into LSPR sensors can provide the highest sensitivity achievable by a plasmon-based biosensor and the detection limits with a wider range of analyte concentrations versus gold nanoparticle aggregation assays. An equally appealing aspect of LSPR-based sensors, like the one described in this study, is that detection is carried out by measurements using a basic hand-held UV–vis spectrophotometer, versus the high cost of equipment and supplies normally associated with SPR. Although SPR spectroscopy provides much higher sensitivity to changes in the bulk refractive index than LSPR spectroscopy, the response of the two techniques becomes comparable when measuring short-range changes in the refractive index due to a molecular adsorption layer. This is a result of the much smaller sensing volume presented by LSPR sensors, because the EM-field-decay length is 40–50 times shorter than that of the SPR sensors. Hence, the sensitivity of LSPR is comparable to SPR for the detection of adsorbed molecules in a 5–15-nm region above the substrate surface. Because of its low detection volume, LSPR measurement is not very sensitive to temperature changes as is the case with SPR. Thus, biosensors based on an LSPR format like the one described here can be used at varying ambient temperatures usually found in laboratory, hospital, or field settings.

Acknowledgement

The authors gratefully acknowledge funding from the National Science Foundation, grant CBET-0854105 (D.S.) and grant 103575 (J.H.); and the Robert A. Welch Foundation grant C-1761 (J.H.).

Journal of Molecular Recognition

REFERENCES

Anker JN, Hall WP, Lyandres O, Shah NC, Zhao J, Van Duyne RP. 2008. Biosensing with plasmonic nanosensors. *Nat. Mater.* **7**: 442–453.

Baker BR, Lai RY, Wood MS, Doctor EH, Heeger AJ, Plaxco KW. 2006. An electronic aptamer-based small molecule sensor for the rapid, label-free detection of cocaine in adulterated samples and biological fluids. *J. Am. Chem. Soc.* **128**: 3138–3139.

Balamurugan S, Obubuafo A, Soper SA, McCarley RL, Spivak DA. 2006. Designing highly specific biosensing surfaces using aptamer monolayers on gold. *Langmuir* **22**: 6446–6453.

Balamurugan S, Obubuafo A, Soper SA, Spivak DA. 2008a. Surface immobilization methods for aptamer diagnostic applications. *Anal. Bioanal. Chem.* **390**: 1009–1021.

Balamurugan S, Obubuafo A, McCarley RL, Soper SA, Spivak DA. 2008b. Effect of linker structure on surface density of aptamer monolayers and their corresponding protein binding efficiency. *Anal. Chem.* **80**: 9630–9634.

Bock LC, Griffin LC, Latham JA, Vermaas EH, Toole JJ. 1992. Selection of single-stranded DNA molecules that bind and inhibit human thrombin. *Nature* **355**: 564–566.

Brody EN, Gold L. 2000. Aptamers as therapeutic and diagnostic agents. *Rev. Mol. Biotechnol.* **74**: 5–13.

Ellington AD, Szostak JW. 1990. In vitro selection of RNA molecules that bind specific ligands. *Nature* **346**: 818–822.

Endo T, Yamamura S, Nagatani N, Morita Y, Takamura Y, Tamiya E. 2005. Localized surface plasmon resonance based optical biosensor using surface modified nanoparticle layer for label free monitoring of antigen–antibody reaction. *Sci. Technol. Adv. Mater.* **6**: 491–500.

Endo T, Kerman K, Nagatani N, Hiepa HM, Kim D-K, Yonezawa Y, Nakano K, Tamiya E. 2006. Multiple label-free detection of antigen-antibody reaction using localized surface plasmon resonance-based core-shell structured nanoparticle layer nanochip. *Anal. Chem.* **78**: 6465–6475.

Gao J, Bender CM, Murphy CJ. 2003. Dependence of the gold nanorod aspect ratio on the nature of the directing surfactant in aqueous solution. *Langmuir* **19**: 9065–9070.

Guo L, Kim D-H. 2011. Reusable plasmonic aptasensors: using a single nanoparticle to establish a calibration curve and to detect analytes. *Chem. Comm.* **47**: 7125–7127.

Guo L, Zhou X, Kim D-H. 2011a. Facile fabrication of distance-tunable Au-nanorod chips for single-nanoparticle plasmonic biosensors. *Biosens. Bioelectron.* **26**: 2246–2251.

Guo L, Ferhan AR, Lee K, Kim D-H. 2011b. Nanoarray-based biomolecular detection using individual Au nanoparticles with minimized localized surface plasmon resonance variations. *Anal. Chem.* **83**: 2605–2612.

Haes AJ, Van Duyne RP. 2004. Preliminary studies and potential applications of localized surface plasmon resonance spectroscopy in medical diagnostics. *Expert Rev. Mol. Diagn.* **4**: 527–537.

Haes AJ, Zou S, Schatz GC, Van Duyne RP. 2004. Nanoscale optical biosensor: short range distance dependence of the localized surface plasmon resonance of noble metal nanoparticle. *J. Phys. Chem. B* **108**: 6961–6968.

Jayasena SD. 1999. Aptamers: an emerging class of molecules that rival antibodies in diagnostics. *Clin. Chem.* **45**: 1628–1650.

Jung LS, Campbell CT, Chinowsky TM, Mar MN, Yee SS. 1998. Quantitative interpretation of the response of surface plasmon resonance sensors to adsorbed films. *Langmuir* **14**: 5636–5648.

Kim D-K, Kerman K, Hiep HM, Saito M, Yamamura S, Takamura Y, Kwon Y-S, Tamiya E. 2008. Label-free optical detection of aptamer-protein interactions using gold-capped oxide nanostructures. *Anal. Biochem.* **379**: 1–7.

Kitano H, Anraku Y, Shinohara H. 2006. Sensing capabilities of colloidal gold monolayer modified with a phenylboronic acid-carrying polymer brush. *Biomacromolecules* **7**: 1065–1071.

Lamont EA, He L, Warriner K, Labuza TP, Sreevatsan S. 2011. A single DNA aptamer functions as a biosensor for ricin. *Analyst* **136**: 3884–3895.

Lee S, Mayer KM, Hafner JH. 2009. Improved localized surface plasmon resonance immunoassay with gold bipyramid substrates. *Anal. Chem.* **81**: 4450–4455.

Liao H, Hafner JH. 2005. Gold nanorod bioconjugates. *Chem. Mater.* **17**: 4636–4641.

Liao H, Nehl CL, Hafner JH. 2006. Biomedical applications of plasmon resonant metal nanoparticles. *Nanomedicine* **1**: 201–208.

Lin T-J, Huang K-T, Liu C-Y. 2006. Determination of organophosphorous pesticides by a novel biosensor based on localized surface plasmon resonance. *Biosens. Bioelectron.* **22**: 513–518.

Liu M, Guyot-Sionnest P. 2005. Mechanism of silver(I)-assisted growth of gold nanorods and bipyramids. *J. Phys. Chem. B* **109**: 22192–22200.

Marinakos SM, Chen S, Chilkoti A. 2007. Plasmonic detection of a model analyte in serum by a gold nanorod sensor. *Anal. Chem.* **79**: 5278–5283.

Mayer KM, Hafner JH. 2011. Localized surface plasmon resonance sensors. *Chem. Rev.* **111**: 3828–3857.

Mayer KM, Lee S, Liao H, Rostro BC, Fuentes A, Scully PT, Nehl CL, Hafner JH. 2008. A label-free immunoassay based upon localized surface plasmon resonance of gold nanorods. *ACS Nano* **2**: 687–692.

Mayer KM, Hao F, Lee S, Nordlander P, Hafner JH. 2010. A single molecule immunoassay by localized surface plasmon resonance. *Nanotechnology* **21**: 255503/1–255503/8.

Meyer C, Hahn U, Rentmeister A. 2011. Cell-specific aptamers as emerging therapeutics. *J. Nucleic Acids* 904750. DOI: 10.4061/2011/904750

Millstone JE, Georganopoulou DG, Xu X, Wei W, Li S, Mirkin CA. 2008. DNA-gold triangular nanoprism conjugates. *Small* **4**: 2176–2180.

Nath N, Chilkoti A. 2002. A colorimetric gold nanoparticle sensor to interrogate biomolecular interactions in real time on a surface. *Anal. Chem.* **74**: 504–509.

Nikoobakht B, El-Sayed MA. 2003. Preparation and growth mechanism of gold nanorods (NRs) using seed-mediated growth method. *Chem. Mater.* **15**: 1957–1962.

Nimjee SM, Rusconi CP, Sullenger BA. 2005. Aptamers: an emerging class of therapeutics. *Annu. Rev. Med.* **56**: 555–583.

Nusz GJ, Marinakos SM, Curry AC, Dahlin A, Hoeoek F, Wax A, Chilkoti A. 2008. Label-free plasmonic detection of biomolecular binding by a single gold nanorod. *Anal. Chem.* **80**: 984–989.

Qin H, Ren J, Wang J, Luedtke NW, Wang E. 2010. G-Quadruplex-modulated fluorescence detection of potassium in the presence of a 3500-fold excess of sodium ions. *Anal. Chem.* **82**: 8356–8360.

Sau TK, Murphy CJ. 2004. Room temperature, high-yield synthesis of multiple shapes of gold nanoparticles in aqueous solution. *J. Am. Chem. Soc.* **126**: 8648–8649.

Sau TK, Murphy CJ. 2005. Self-assembly patterns formed upon solvent evaporation of aqueous cetyltrimethylammonium bromide-coated gold nanoparticles of various shapes. *Langmuir* **21**: 2923–2929.

Song S, Wang L, Li J, Fan C, Zhao J. 2008. Aptamer-based biosensors. *Trends Anal. Chem.* **27**: 108–117.

Storhoff JJ, Elghanian R, Mucic RC, Mirkin CA, Letsinger RL. 1998. One-pot colorimetric differentiation of polynucleotides with single base imperfections using gold nanoparticle probes. *J. Am. Chem. Soc.* **120**: 1959–1964.

Tuerk C, Gold L. 1990. Systematic evolution of ligands by exponential enrichment: RNA ligands to bacteriophage T4 DNA polymerase. *Science* **249**: 505–510.

Yasun E, Gulbakan B, Ocsoy I, Yuan Q, Shukoor MI, Li C, Tan W. 2012. Enrichment and detection of rare proteins with aptamer-conjugated gold nanorods. *Anal. Chem.* **84**: 6008–6015.

Yonzon CR, Jeoung E, Zou S, Schatz GC, Mrksich M, Van Duyne RP. 2004. A comparative analysis of localized and propagating surface plasmon resonance sensors: the binding of concanavalin A to a monosaccharide functionalized self-assembled monolayer. *J. Am. Chem. Soc.* **126**: 12669–12676.

Yu C, Irudayaraj J. 2007. Multiplex biosensor using gold nanorods. *Anal. Chem.* **79**: 572–579.

Zhao J, Zhang X, Yonzon CR, Haes AJ, Van Duyne RP. 2006. Localized surface plasmon resonance biosensors. *Nanomedicine* **1**: 219–228.

